

Supporting Information for

Temperature-Dependent Lipid Extraction from Membranes by Boron Nitride Nanosheets

Zhen Li,[†] Yonghui Zhang,[†] Chun Chan,[†] Chunyi Zhi,^{†*} Xiaolin Cheng,^{‡*} and Jun Fan^{†¶⊥*}

[†]Department of Materials Science and Engineering, City University of Hong Kong, Hong Kong, China

[‡]Division of Medicinal Chemistry and Pharmacognosy, College of Pharmacy, The Ohio State University, Columbus, Ohio, United States of America

[¶]City University of Hong Kong Shenzhen Research Institute, Shenzhen 518057, China

[⊥]Center for Advanced Nuclear Safety and Sustainable Development, City University of Hong Kong, Hong Kong, China

*E-mails: cy.zhi@cityu.edu.hk (Chunyi Zhi), cheng.1302@osu.edu (Xiaolin Cheng), and junfan@cityu.edu.hk (Jun Fan)

Contents:

SI-1: Experimental Confirmation of the Lipid Adsorption onto BN Surfaces

SI-2: Additional MD Results for the Lipid Extraction from POPC and DMPC Membranes

SI-3: BN Docking Models

SI-4: Adsorption of DMPC on BN Surfaces at High/Low Temperature in Experiments

SI-5: Temperature-Dependent Lipid Extraction from *Escherichia coli* Membranes

SI-6: Additional Phase Analyses for POPC and DMPC Membranes at Different Temperatures

SI-7: Reasonability of Restraining BN Models

SI-8: The Convergence Test for PMF Results

References

SI-1: Experimental Confirmation of the Lipid Adsorption onto BN Surfaces

To further verify the attraction and adsorption of lipids onto the surface of boron nitride (BN) nanosheets, BN plates were prepared in experiment and the adsorption of lipids was tested with electron energy loss spectroscopy (EELS) and energy dispersive spectroscopy (EDS). Specifically, BN plates were polished to expose their fresh surfaces consisting of micro-sized BN platelets; 0.2 mg lipids were dispersed into 2 ml deionized water by strong sonication, and sealed and placed in oven for 1 hour. Then, the polished BN plates were dipped into the lipid dispersions, followed by sealing and placing in oven for over 48 hours. After that, the BN plates were taken out, rinsed in deionized water, and dried for testing.

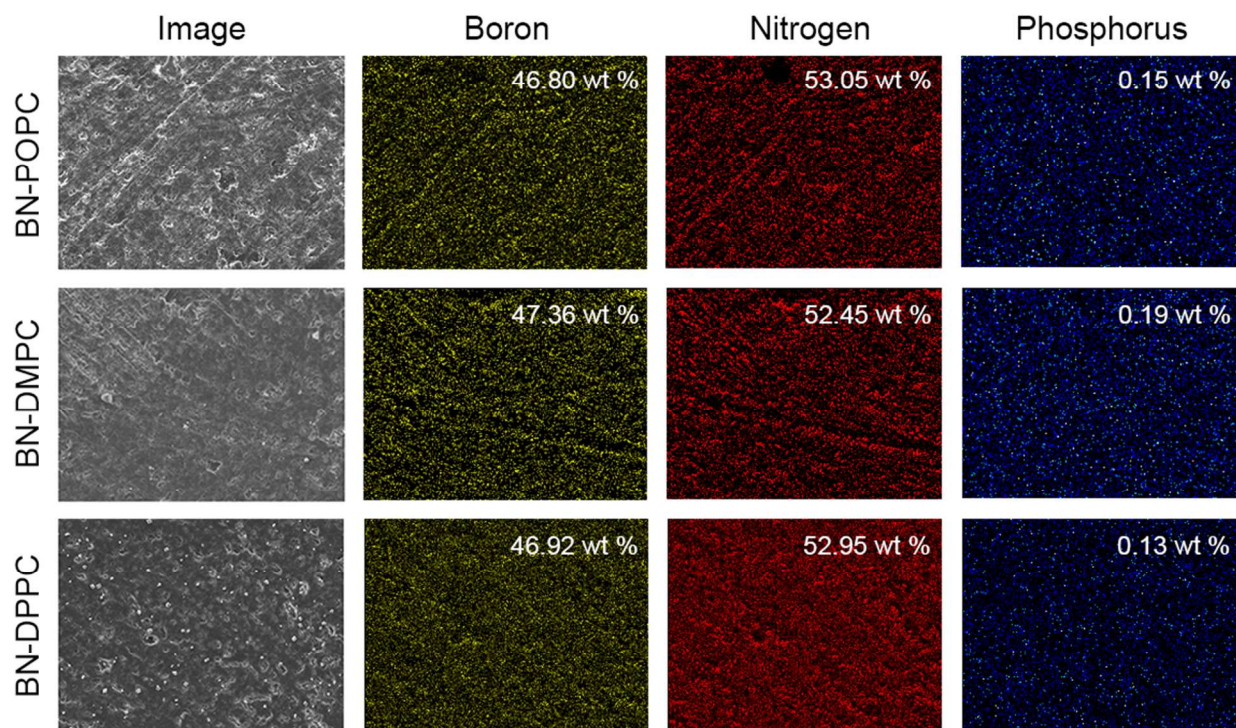


Figure S1. Experimental results confirm the adsorption of lipids onto the surface of BN nanosheets. The left column shows the SEM images of BN plates. The right three columns show the EELS mapping of boron, nitrogen, and phosphorus elements on the BN plates. The normalized weight percentage of boron, nitrogen, and phosphorus were obtained using EDS and labelled on the EELS mappings.

Not only POPC but also another two kinds of lipids (DMPC and DPPC) were used to perform the experiments. As shown in Figure S1, the BN plates are covered by phosphorus that belongs to lipid molecules, indicating that lipids were extracted from lipid assemblies and adsorbed onto the surface of BN nanosheets. The normalized weight percentage of boron, nitrogen, and phosphorus were also obtained and labelled in Figure S1. In sum, the adsorption of lipids onto the surface of BN nanosheets was experimentally confirmed.

SI-2: Additional MD Results for the Lipid Extraction from POPC and DMPC Membranes

In Figure 1 of the main text, we presented that the boron nitride (BN) nanosheet can extract lipids from the POPC membrane at 290 K. Here, the results of POPC at 300 K and 310 K are supplemented (the left and the middle panels in Figure S1A), which show that the lipid extraction also happens for POPC membranes at 300 K and 310 K. In brief, we observed the lipid extraction from POPC membranes by BN nanosheets at all the three temperatures (290, 300, and 310 K).

Similarly, the lipid extraction was also simulated with DMPC membranes at 290, 300, and 310 K. Results at 290 K and 300 K are presented in Figure 2 of the main text, showing the temperature-dependent characteristic. Here we show that the BN nanosheet can also extract lipids from the DMPC membrane at 310 K (the right panel in Figure S1A). In sum, for DMPC membranes, the lipid extraction happens at 310 K and 300 K, but disappears at 290 K.

To reveal detailed dynamic information, we traced the z-position of the bottom of the BN nanosheets (the bottommost atom of the BN nanosheet in each frame) and the phosphorus atoms in lipids. The results for DMPC at 300 K and 290 K are discussed in the main text (Figure 2BD). In Figure S1B, results for POPC membranes and the DMPC membrane at 310 K are supplemented. Some black lines in Figure S1B go up and down at early stage, showing that the BN nanosheets move randomly. After binding to the lipid membranes, the BN nanosheets gradually extract lipids out and insert into membranes.

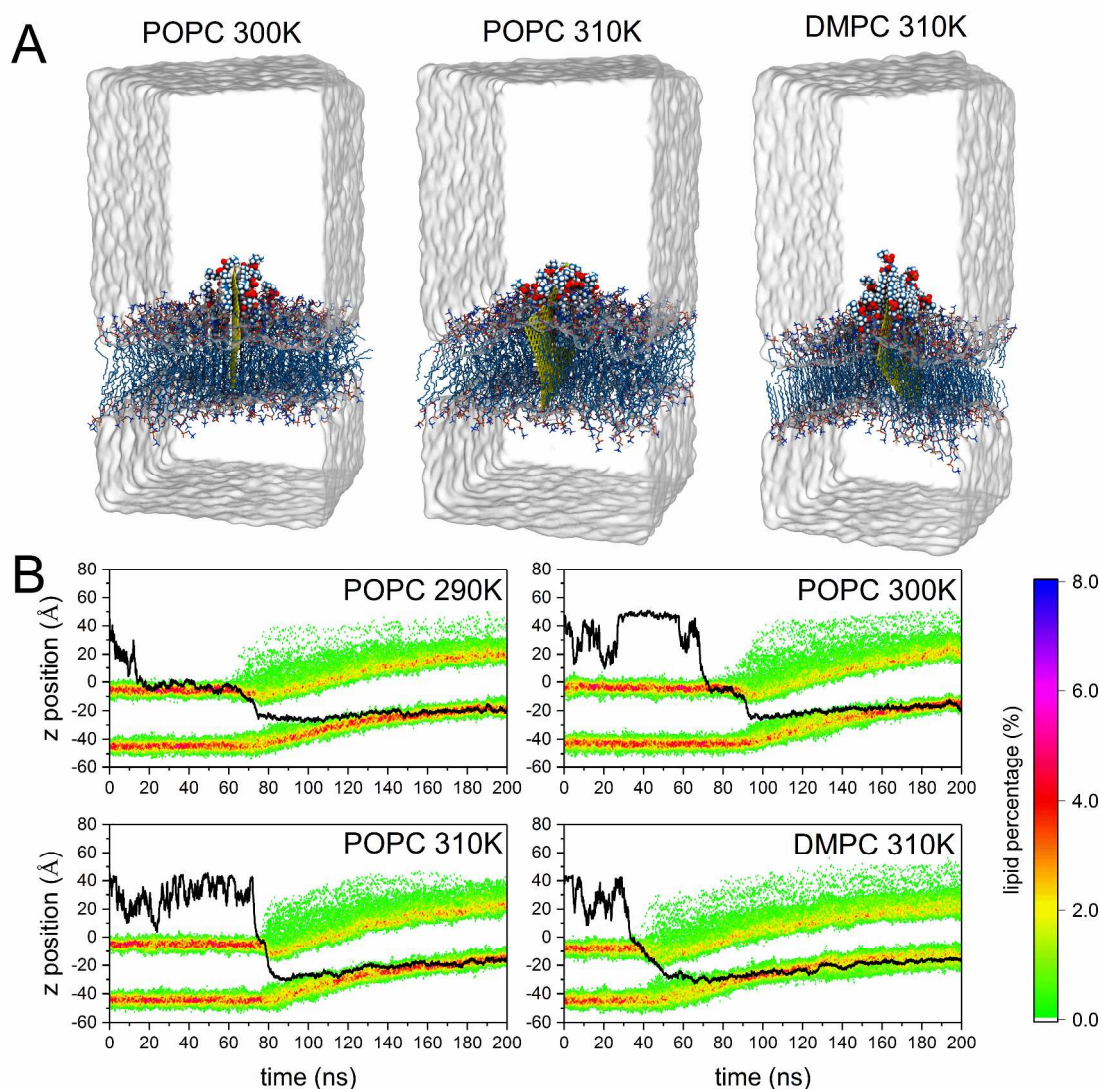


Figure S2. (A) The final snapshots of lipid extraction simulations show that the BN nanosheet can extract lipids from the POPC membrane at 300 and 310 K, and from the DMPC membrane at 310 K. (B) The z-position evolution of the BN nanosheet (black lines) and lipids collected with tracing the bottom of BN nanosheets and phosphorus atoms in lipids. The initial tops of lipid bilayers were taken as zero points along the z axis.

SI-3: BN Docking Models

In above mentioned models (Figure 1 and Figure 2 in the main text, and Figure S1), the BN nanosheets move freely with only an atom at one corner restrained. Because of the computational burden, the size of the BN nanosheet is not large ($\sim 45 \times 45 \text{ \AA}^2$). As a result, the BN nanosheets almost sink into lipid membranes at last, which covers up the lipid extraction phenomenon. To show the lipid extraction more clearly, a larger sized BN nanosheet ($\sim 50 \times 70 \text{ \AA}^2$) was fully restrained and perpendicularly positioned onto lipid membranes. With such BN docking models, we obtained same results as discussed above (Figure S3).

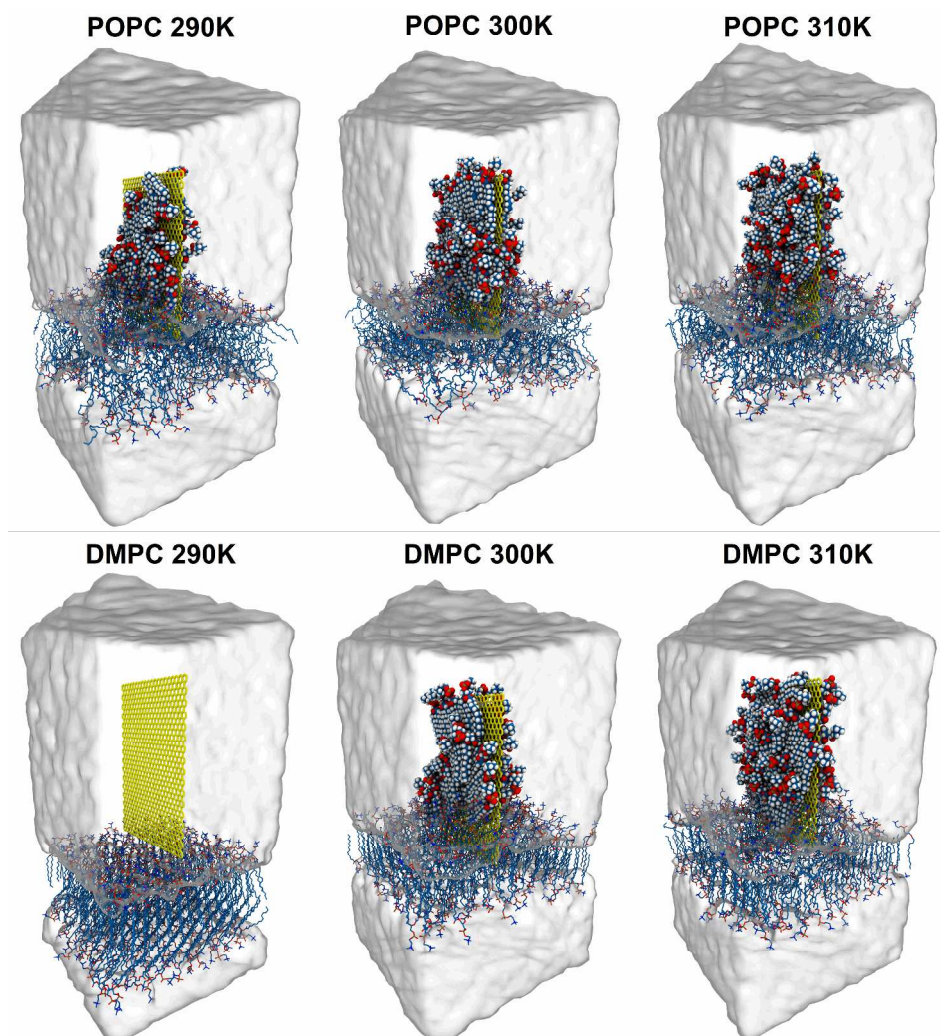


Figure S3. The lipid extraction from POPC and DMPC membranes modeled with fully restrained BN nanosheets.

SI-4: Adsorption of DMPC on BN Surfaces at High/Low Temperature in Experiments

In simulation, we observed that the lipid extraction of DMPC disappears as temperature decreases. To verify it, we performed experiments (as presented in section SI-1) for DMPC at high (45 °C) and low (3 °C) temperatures. At high temperature, there is 0.19 wt % phosphorus on the BN plate measured using EDS; however, at low temperature, no phosphorus can be found on the BN plate. Therefore, the extraction and adsorption of lipids on BN surfaces is temperature-dependent.

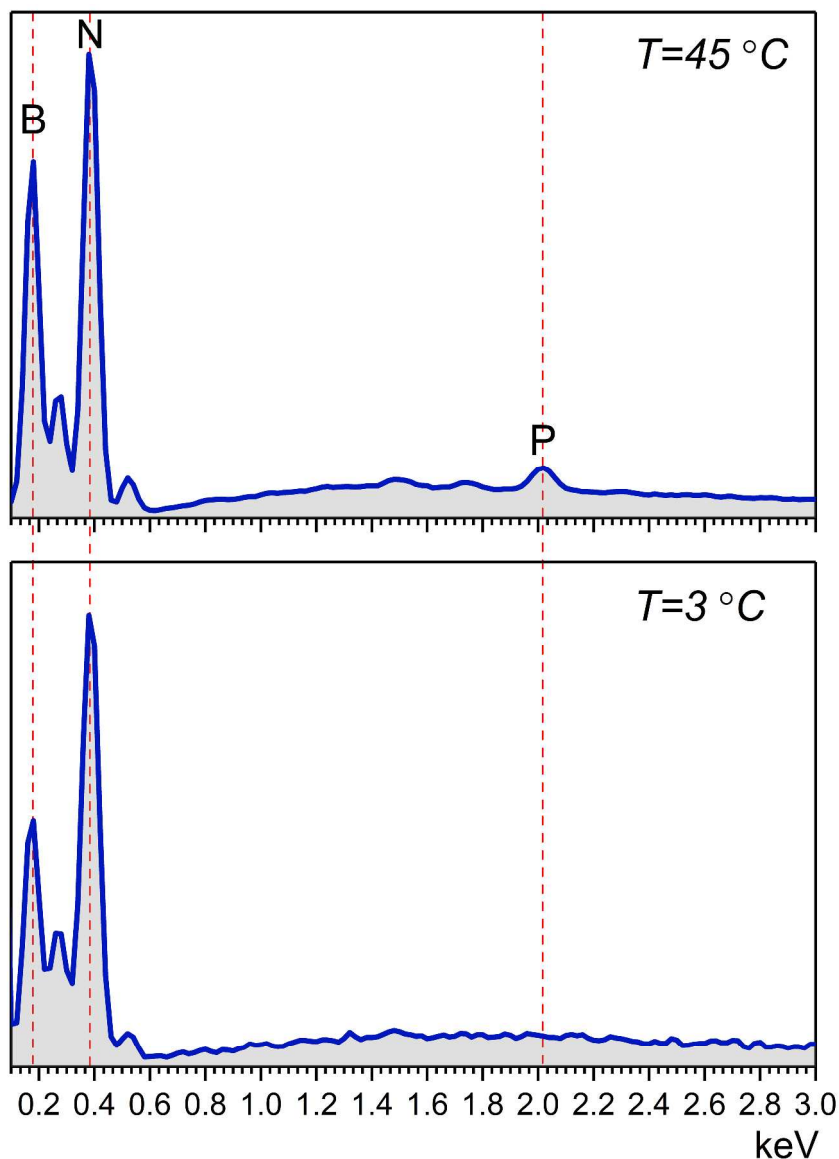


Figure S4. EDS spectrum showing that the extraction of phosphorus (lipids) is temperature-dependent

SI-5: Temperature-Dependent Lipid Extraction from *Escherichia coli* Membranes

The lipid extraction behavior was firstly reported by Tu *et al.*¹ In experiment, they observed that the morphology of *Escherichia coli* can be damaged by graphene nanosheets. Then, they performed molecular dynamics (MD) simulations and found the lipid extraction mechanism. To mimic the inner and outer membranes of *Escherichia coli*, they used POPE and POPG (commonly found lipids in Gram-negative bacteria) to build models. The outer membrane of *Escherichia coli* was modeled with pure POPE, and the inner membrane was modeled with 3:1 mixed POPE and POPG which was also used in other works.^{2,3}

In the work of Tu and coworkers, the lipid extraction was observed at 310 K; but they did not study the effect of temperature, and they did not discuss how to mitigate the lipid extraction. In our models of DMPC, the lipid extraction is temperature dependent. We believed that this temperature dependence is a general characteristic of the lipid extraction even though it happens at all the sample temperatures for POPC. To confirm the universality of the temperature dependence, we also performed simulations with the inner and outer membrane models of *Escherichia coli* according to the work of Tu *et al.*¹

As shown in Figure S5, at 310 K, we observed lipid extraction for both the outer and the inner membranes of *Escherichia coli*, as reported by Tu *et al.*¹ for graphene and graphene oxide. With decreasing the temperature, we also observed the temperature-dependent results (Figure S5). Therefore, the temperature dependence should be a general characteristic of the lipid extraction behavior of 2D materials. The critical temperature varies for lipid membranes of different components as shown in Figure S5, which has been explained in the following part in the main text.

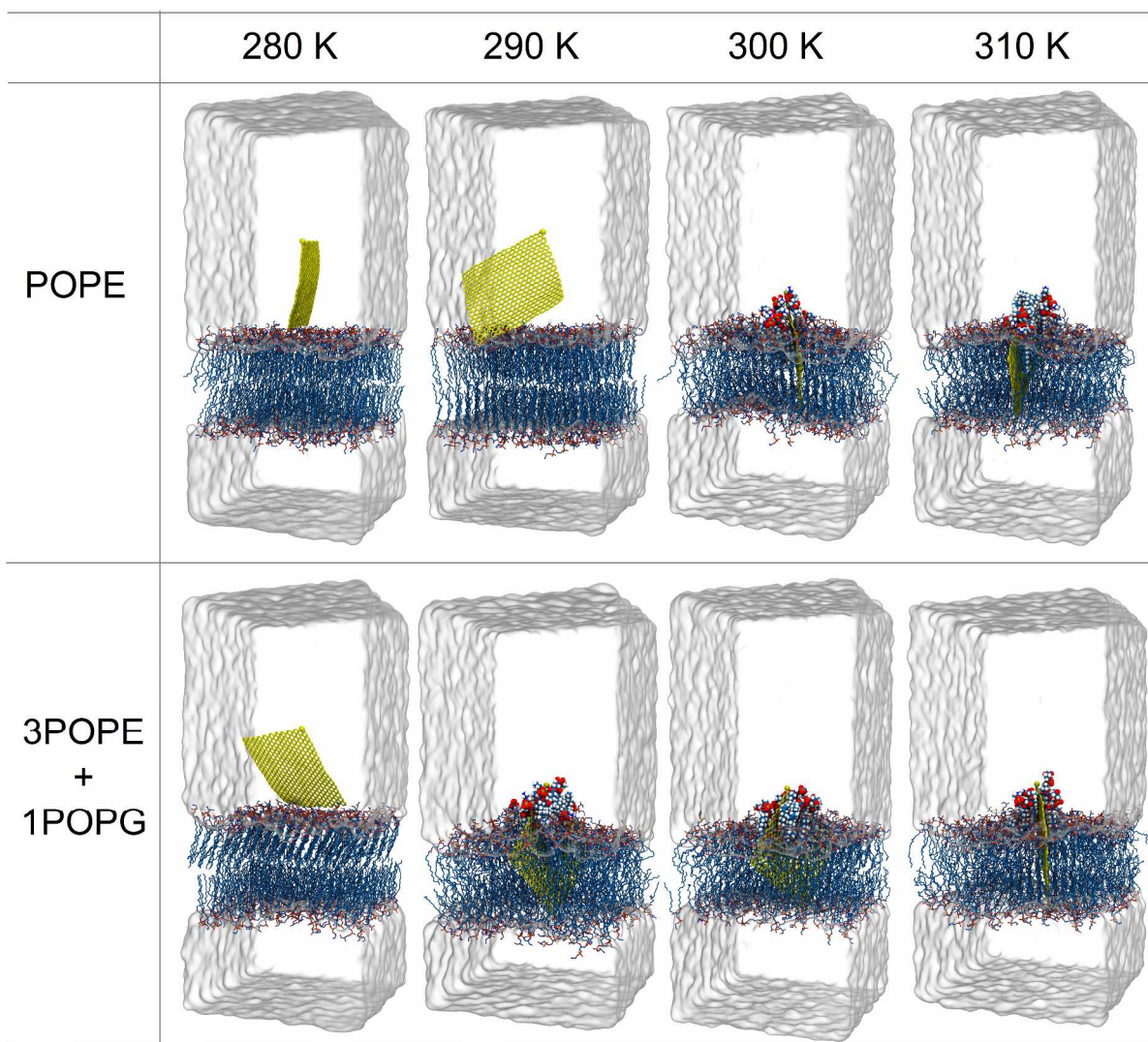


Figure S5. Temperature-dependent lipid extraction of BN nanosheets from the outer membrane (pure POPE) and the inner membrane (3:1 mixed POPE and POPG) of *Escherichia coli*. The lipid extraction phenomenon disappears when decreasing temperature to 290 K and 300 K for the outer membrane and the inner membrane of *Escherichia coli*, respectively.

Please note that the outer membrane of *Escherichia coli* modeled with pure POPE is a drastic simplification. In reality, the outer membrane of *Escherichia coli* is asymmetric bilayer; the outer leaflet is composed of lipopolysaccharide (LPS) molecules (hydrophobic lipid A attached to phosphorylated sugar chains), and the inner leaflet is composed of phospholipids.⁴ The LPS layer definitely would affect the interaction between 2D materials and the membrane, which should be studied in future works using recently developed accurate models.⁴⁻⁷

SI-6: Additional Phase Analyses for POPC and DMPC Membranes at Different Temperatures

For DMPC, when decreasing temperature from 300 K to 290 K, the lipid extraction behavior disappears. With analyzing the structural details of DMPC membranes, we found that the DMPC membrane transitions from liquid phase (at 300 K) to gel phase (at 290 K), as shown in Figure 3 of the main text. Therefore, the temperature dependence of the lipid extraction should be related to the phase state of lipid membranes. Here, supplemented results are shown for POPC and DMPC membranes. The lipid orientation of the DMPC membrane at 310 K and the POPC membrane at 290, 300, and 310 K are all chaotic (Figure S6). Only the slay angle distribution of the DMPC membrane at 290 K is quite narrow (Figure S7), which means a highly ordered phase state.

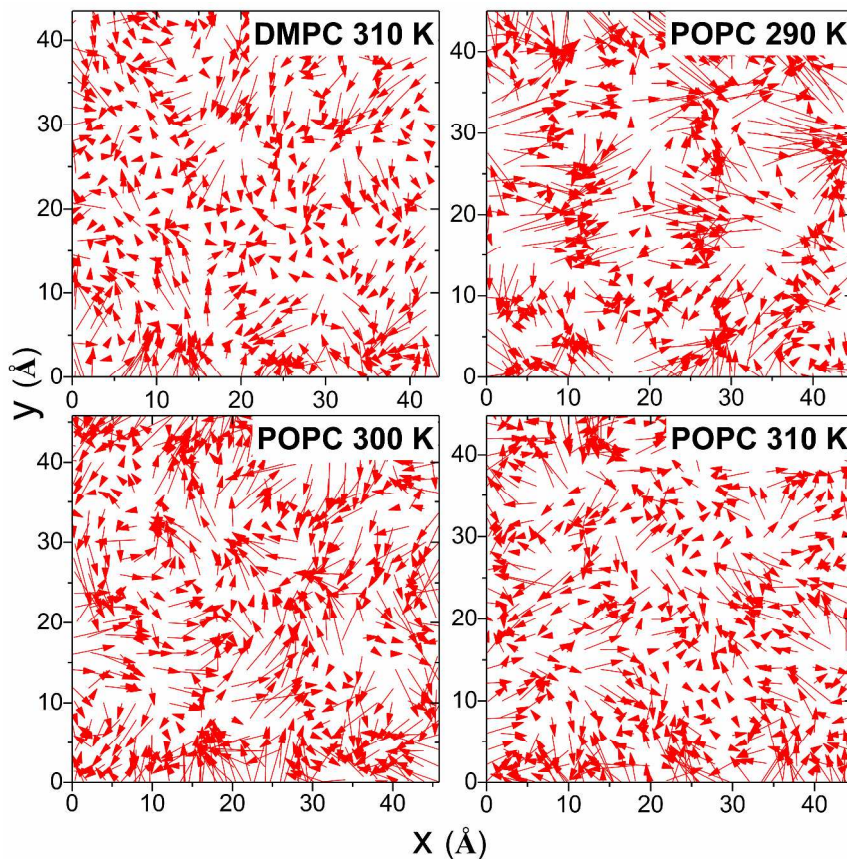


Figure S6. The averaged distribution of lipid head-to-tail (from the phosphorus atom to the two terminal carbon atoms in tails) vectors projected onto the membrane plane for DMPC at 310 K and POPC at 290, 300, and 310 K. They are all chaotic liquid phase states.

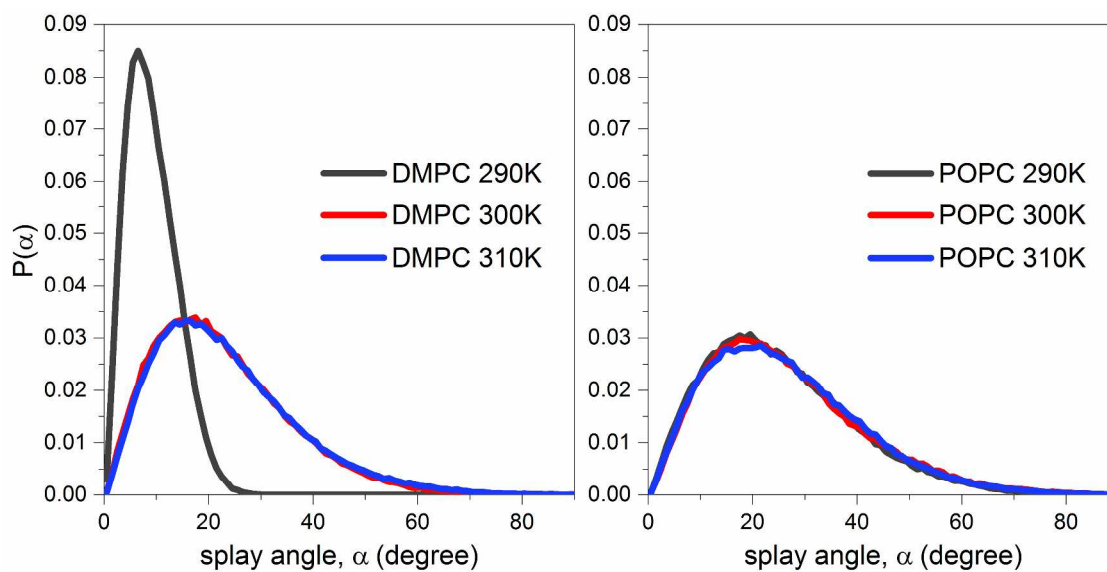


Figure S7. The splay angle distribution of DMPC and POPC membranes at 290, 300, and 310 K, it is normalized probability density of finding a pair of lipids at an angle α with respect to each other.

SI-7: Reasonability of Restraining BN Models

In the models of this work, position restraints were applied to BN models in two modes: (1) restraining an atom at one corner of the BN nanosheet; (2) fully restraining all the atoms of the BN nanosheet. The first mode was adopted for all the models in the main text. The second mode can reduce the computational burden and show the lipid extraction more clearly, which was used in supplemented docking BN simulations as shown in Figure S3.

In surface engineering, 2D materials can be deposited on the surface of materials to obtain antibacterial performance.^{8, 9} In such applications, nanosheets bind substrates firmly, representing a restrained state. Thus, position restrained nanosheets in our simulations mimic these cases reasonably. Such restrained models have been widely used in studying the lipid extraction behavior of 2D materials.^{1, 10-12}

For *in vivo* applications, the case would be complicated; nanosheets can freely move, and the orientation of nanosheets and cell membranes would be random. The fully restrained models (Figure S3) only include the perpendicular orientation. Although the one-atom-restrain models allow the random movements of nanosheets to some extent (see the movie), the nanosheets almost perpendicular to the lipid membranes when binding to them. That is to say, almost only the perpendicular orientation between BN nanosheets and lipid membranes was considered in this work. However, that is enough for the study of the lipid extraction. The simulation work of Li *et al.*¹³ demonstrated that the perpendicular orientation has the lowest energy barrier to pierce lipid membranes; Lu *et al.*⁹ controlled the alignment of graphene oxide nanosheets on the surface of substrates in experiments and they found that vertical nanosheets possess the best antibacterial performance. Therefore, perpendicular nanosheets can damage cell membranes most efficiently; the perpendicular orientation is appropriate to study the lipid extraction behavior of 2D materials.

Taken together, restraining BN nanosheets in our models is appropriate and reasonable to study the lipid extraction of 2D materials. The orientation of nanosheets when interacting with cell membranes could affect the cytotoxicity of nanosheets as studied by Lu and coworkers,⁹ the molecular details of which should be further investigated with MD simulations.

SI-8: The Convergence Test for PMF Results

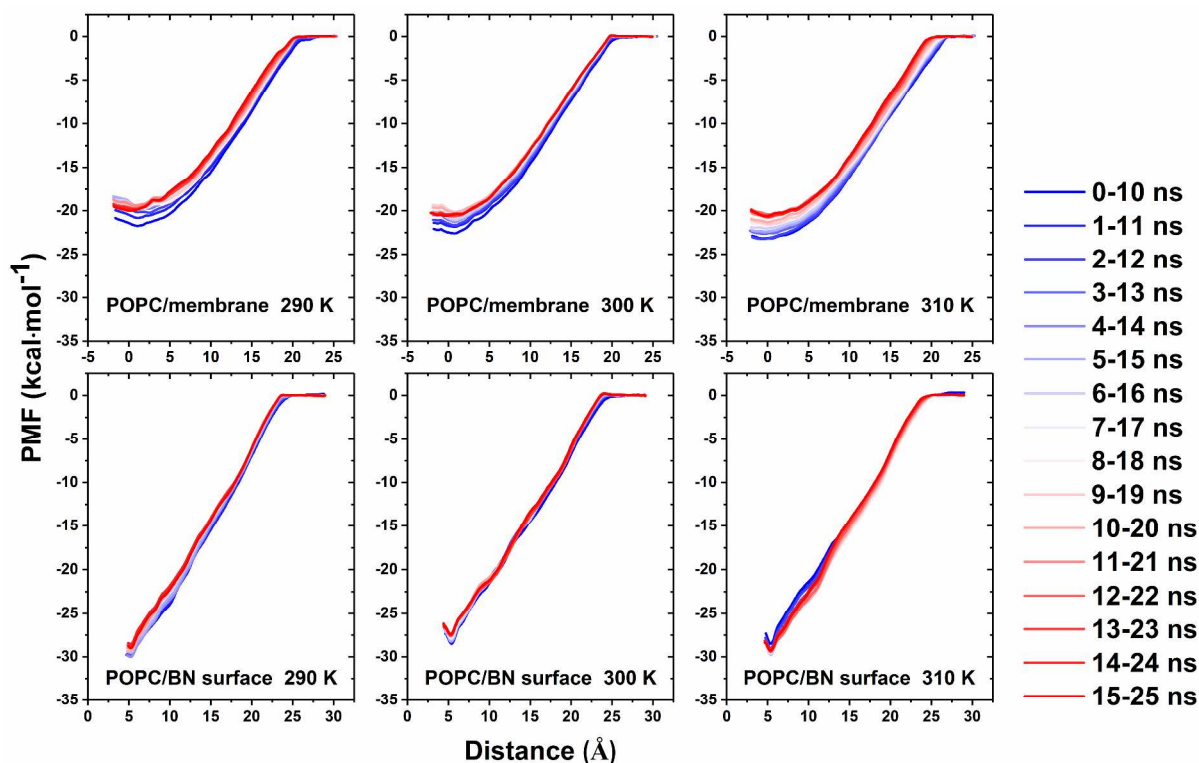


Figure S8. Potential of mean force (PMF) convergence testing for pulling a POPC lipid away from the POPC membrane and from the BN surface. PMF profiles were calculated for 10 ns time intervals every 1 ns, and colored from blue to red. Evolution of PMF profiles shows that the results reached convergence at 15-25 ns. The distance (x-axis) between POPC and the membrane is the z distance from the center-of-mass of phosphorus atoms in upper leaflets of membranes to the pulled phosphorus atom. The distance between POPC and the BN surface is the z distance from the center-of-mass of BN nanosheet to the pulled phosphorus atom.

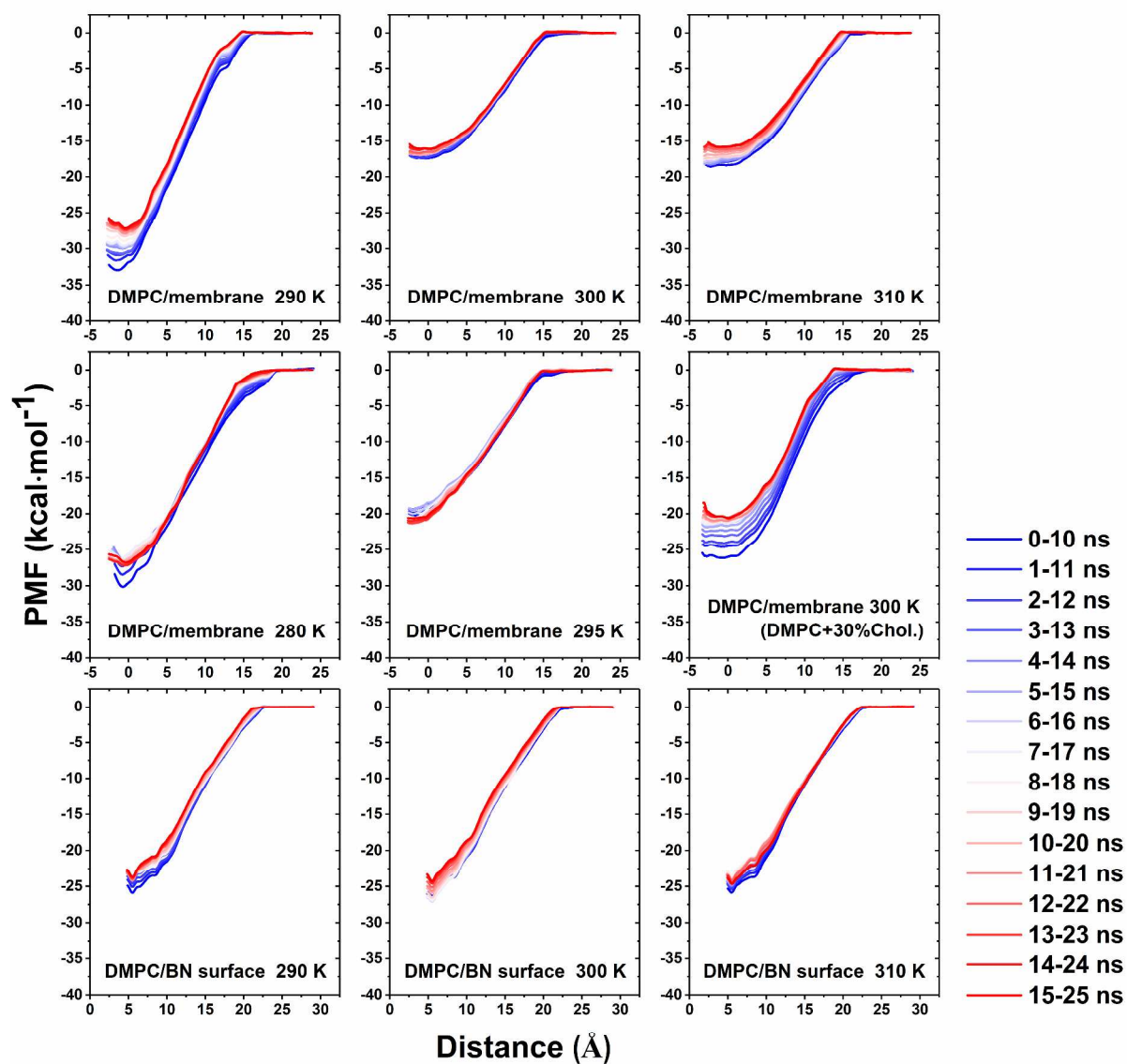


Figure S9. PMF convergence testing for pulling a DMPC lipid away from DMPC membranes and from the BN surface. Similarly, the distance (x-axis) between DMPC and membranes is the z distance from the center-of-mass of phosphorus atoms in upper leaflets of membranes to the pulled phosphorus atom. The distance between DMPC and the BN surface is the z distance from the center-of-mass of the BN nanosheet to the pulled phosphorus atom.

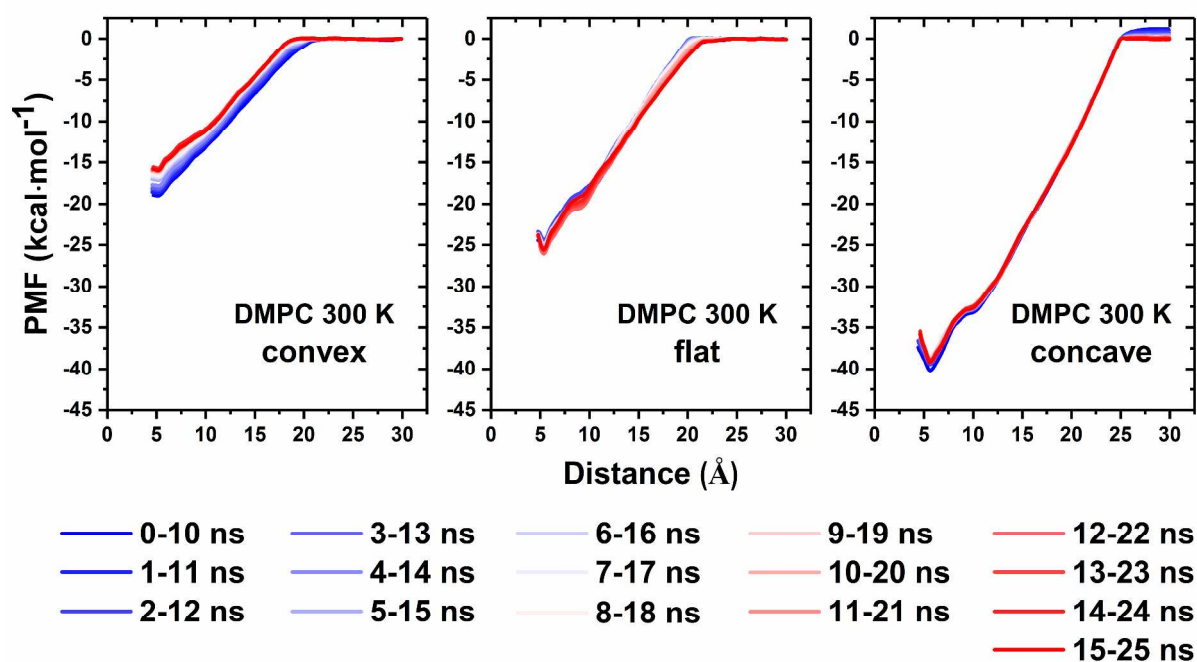


Figure S10. PMF convergence testing for pulling a DMPC lipid away from curved BN surfaces at 300 K. The distance between DMPC and BN surfaces is measured from the pulled phosphorus atom to an atom at the vault of the (10, 10) nanotube.

References

- (1) Tu, Y.; Lv, M.; Xiu, P.; Huynh, T.; Zhang, M.; Castelli, M.; Liu, Z.; Huang, Q.; Fan, C.; Fang, H.; Zhou, R. Destructive Extraction of Phospholipids from *Escherichia coli* Membranes by Graphene Nanosheets. *Nat. Nanotechnol.* **2013**, *8*, 594–601.
- (2) Murzyn, K.; Róg, T.; Pasenkiewicz-Gierula, M. Phosphatidylethanolamine-Phosphatidylglycerol Bilayer as a Model of the Inner Bacterial Membrane. *Biophys. J.* **2005**, *88*, 1091–1103.
- (3) Zhao, W.; Róg, T.; Gurtovenko, A. A.; Vattulainen, I.; Karttunen, M. Role of Phosphatidylglycerols in the Stability of Bacterial Membranes. *Biochimie* **2008**, *90*, 930–938.
- (4) Clifton, L. A.; Holt, S. A.; Hughes, A. V.; Daulton, E. L.; Arunmanee, W.; Heinrich, F.; Khalid, S.; Jefferies, D.; Charlton, T. R.; Webster, J. R. P.; Kinane, C. J.; Lakey, J. H. An Accurate *In Vitro* Model of the *E. coli* Envelope. *Angew. Chem., Int. Ed.* **2015**, *54*, 11952–11955.
- (5) Wu, Emilia L.; Fleming, Patrick J.; Yeom, Min S.; Widmalm, G.; Klauda, Jeffery B.; Fleming, Karen G.; Im, W. *E. coli* Outer Membrane and Interactions with OmpLA. *Biophys. J.* **2014**, *106*, 2493–2502.
- (6) Hsu, P.-C.; Jefferies, D.; Khalid, S. Molecular Dynamics Simulations Predict the Pathways *via* Which Pristine Fullerenes Penetrate Bacterial Membranes. *J. Phys. Chem. B* **2016**, *120*, 11170–11179.
- (7) Berglund, N. A.; Piggot, T. J.; Jefferies, D.; Sessions, R. B.; Bond, P. J.; Khalid, S. Interaction of the Antimicrobial Peptide Polymyxin B1 with Both Membranes of *E. coli*: A Molecular Dynamics Study. *PLoS Comput. Biol.* **2015**, *11*, e1004180.
- (8) Akhavan, O.; Ghaderi, E. Toxicity of Graphene and Graphene Oxide Nanowalls against Bacteria. *ACS Nano* **2010**, *4*, 5731–5736.
- (9) Lu, X.; Feng, X.; Werber, J. R.; Chu, C.; Zucker, I.; Kim, J.-H.; Osuji, C. O.; Elimelech, M. Enhanced Antibacterial Activity through the Controlled Alignment of Graphene Oxide Nanosheets. *Proc. Natl. Acad. Sci.* **2017**, *114*, E9793–E9801.
- (10) Gu, Z.; Yang, Z.; Luan, B.; Zhou, X.; Hong, L.; Zhou, H.; Luo, J.; Zhou, R. Membrane Insertion and Phospholipids Extraction by Graphyne Nanosheets. *J. Phys. Chem. C* **2017**, *121*, 2444–2450.
- (11) Luan, B.; Zhou, S.; Wang, D.; Zhou, R. Detecting Interactions between Nanomaterials and Cell Membranes by Synthetic Nanopores. *ACS Nano* **2017**, *11*, 12615–12623.
- (12) Zhang, L.; Xu, B.; Wang, X. Cholesterol Extraction from Cell Membrane by Graphene Nanosheets: A Computational Study. *J. Phys. Chem. B* **2016**, *120*, 957–964.
- (13) Li, Y.; Yuan, H.; von dem Bussche, A.; Creighton, M.; Hurt, R. H.; Kane, A. B.; Gao, H. Graphene Microsheets Enter Cells through Spontaneous Membrane Penetration at Edge Asperities and Corner Sites. *Proc. Natl. Acad. Sci.* **2013**, *110*, 12295–12300.